AXIAL LOAD FAILURE OF SHEAR CRITICAL COLUMNS SUBJECTED TO HIGH LEVELS OF AXIAL LOAD

A.B. Matamoros[1], Lisa Matchulat[2], and Charles Woods[3]

[1] *Associate Professor, CEAE Dept., University of Kansas, Lawrence, KS, USA*

[2] *Graduate Research Assistant, CEAE Dept., University of Kansas, Lawrence, KS, USA*
Email: abm@ku.edu, lmatch@ku.edu, cjwoods@ku.edu

ABSTRACT :

This paper discusses the experimental behavior of two lightly reinforced (shear-critical) columns subjected to high levels of axial load and lateral load reversals. The two full-scale experiments were carried out at the NEES-MAST facility at the University of Minnesota as part of a large study on the risk of collapse of older concrete buildings during major earthquakes. The goal of the experiments was to obtain data to improve simulations of buildings in which partial collapse and redistribution of vertical loads between columns takes place. Tests evaluated the behavior of two columns with ratios of nominal shear strength to plastic shear demand on the order of 0.85. The longitudinal and transverse reinforcement ratios were maintained constant, while the axial load ratio of each column was 0.3 and 0.2 $f'_c A_g$, respectively.

The two columns had a height of 2945 mm and cross section of 457 x 457 mm. The longitudinal reinforcement ratio was 2.5% and the transverse reinforcement consisted to No. 3 bars (9.5 mm diameter) spaced at a distance equivalent to the column size (457 mm). The loading protocol consisted of cycles with increasing maximum lateral displacement under constant axial load. It was found that the behavior of the two columns at drift demands higher than the drift at axial failure was significantly different. The lateral stiffness and the residual axial load capacity of the columns were found to be related to the axial load prior to axial failure.

KEYWORDS: Column, reinforced concrete, collapse, shear, axial failure

1. INTRODUCTION

Seismic evaluation and rehabilitation of older reinforced concrete buildings is a very difficult process because it requires modeling the behavior of heavily damaged reinforced concrete elements. Furthermore, in order to simulate the behavior of a building until collapse of the gravity load resisting system, it may be necessary to simulate the behavior of some column elements after they lose the capacity to carry axial loads.

This paper investigates the behavior of the type of column elements most vulnerable to sudden axial failure. Those are columns subjected to high levels of axial load in which the lateral load capacity is limited by the shear strength. The goals of the research were to improve the understanding about the behavior of these column elements and to obtain new experimental data about the behavior of these elements at deformations beyond those that cause them to lose their ability to carry gravity loads.

2. EXPERIMENTAL PROGRAM

The experimental program consisted of two full-scale columns with square-cross-section. Columns (Fig. 1) were tested at the NEES-MAST Laboratory at the University of Minnesota. A full description of the capabilities of the testing system may be found elsewhere (University of Minnesota, 2008). Both specimens had a length of 2945 mm and cross-section dimensions of 457 x 457 mm, for a shear-span to depth ratio of 3.75. The longitudinal reinforcement consisted of 8 No. 9 bars (28.7 mm diameter) made of ASTM A706 steel with a measured yield strength of 445 MPa. Transverse reinforcement consisted of No. 3 bars (9.5 mm diameter) made of ASTM A615 steel with a yield strength of 372 MPa. Transverse reinforcement consisted of closed hoops with 90 deg. bends spaced at 457 mm. Compressive strength of the concrete measured on the day of the test for the two specimens was 33 MPa.

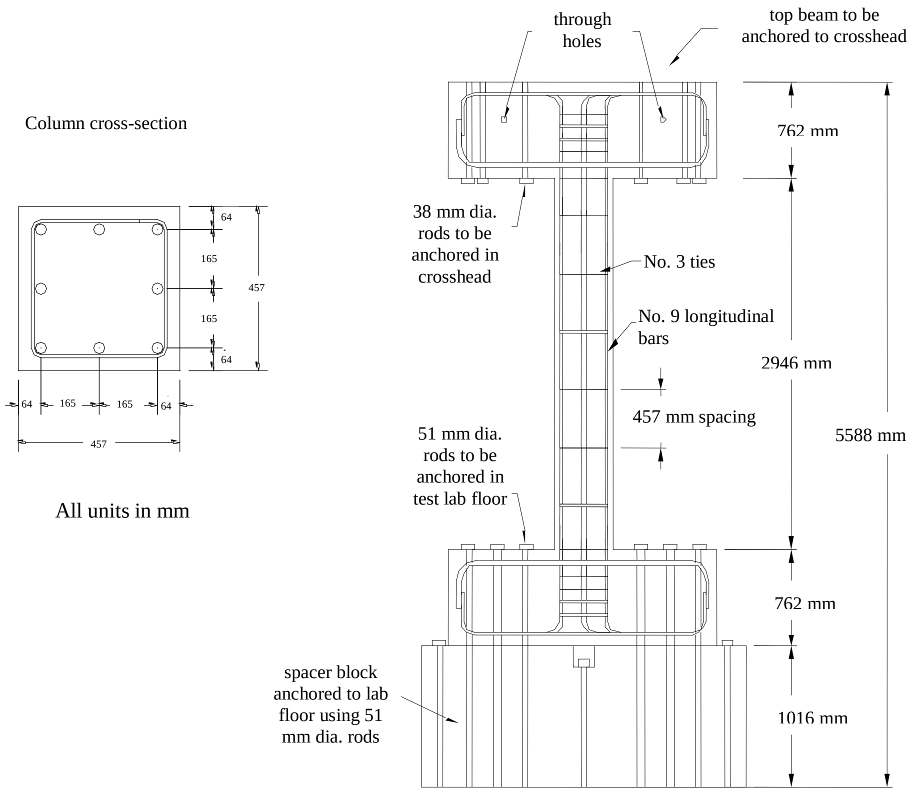

Figure 1 Specimen dimensions

2.1. Loading Protocol

Specimens were subjected to sets of three cycles with increasing displacement (Fig.2). The amplitude of each set of cycles was increased by 0.25% up to a drift ratio of 1.5%, and by 0.5% increments after that. Axial load remained constant with values of 2225 KN and 1510 KN for specimens 1 and 2, respectively. These values correspond to axial load ratios of 0.32 and 0.21.

The control system was configured to switch from load control to displacement control in the vertical actuators if a reduction of 10% or greater was detected in the axial load capacity. The system was programmed to maintain the lateral and vertical deformation constant after the triggering criteria was met. This was designated as an axial failure event. After each failure event, the control system was transitioned from displacement to load control in the axial direction, but under the reduced axial load recorded at the end of the failure event. After the axial load in the column was stabilized, the displacement protocol for the lateral deformation was continued.

The loading protocol changed when damage to the columns was deemed too severe. At that point the vertical deformation was increased while maintaining the maximum lateral displacement recorded in the column constant. This was intended to obtain a measure of the residual axial capacity of the column.

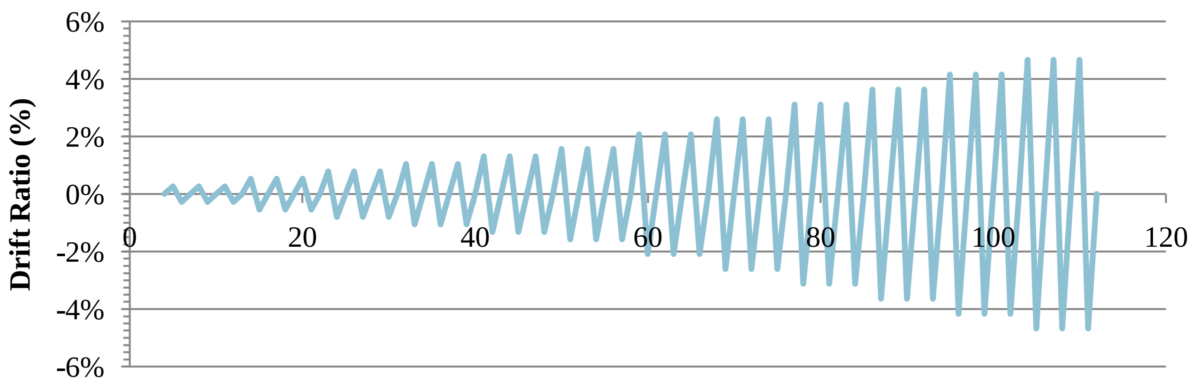

Figure 2 Lateral displacement protocol

3. EXPERIMENTAL RESULTS

The behavior of both specimens was very brittle in nature. For specimen 1 axial failure occurred at a drift ratio of 1.07%. Failure occurred after rapid widening of an existing shear crack (Fig. 3a and 3b), followed by sudden loss in axial capacity. The inclined crack associated with axial failure formed in the maximum moment region, on the bottom side the specimen, and formed an angle of approximately 28 deg. with respect to the vertical axis of the column. Failure of specimen 2 was similar in nature. Axial failure was recorded at a drift ratio of 1.2% and it was precipitated by the appearance of a previously inexistent inclined crack in the middle section of the column (Fig. 3c). In the case of specimen 2 the crack formed a much shallower angle of approximately 14 deg. with respect to the vertical axis (Fig. 3c).

Hysteresis curves for both specimens are presented in Fig. 4. The hysteretic response shows that both specimens failed prior to any significant yielding in flexure and that the ability to dissipate energy was negligible. Although the hysteresis curves show similar behavior for both columns, there were important differences in terms of the axial deformation, lateral stiffness, and residual strength that will be discussed in latter sections.

Figure 3. (a) Specimen 1 prior to axial failure (b) Specimen 1 after axial failure (c) Specimen 2 after axial failure

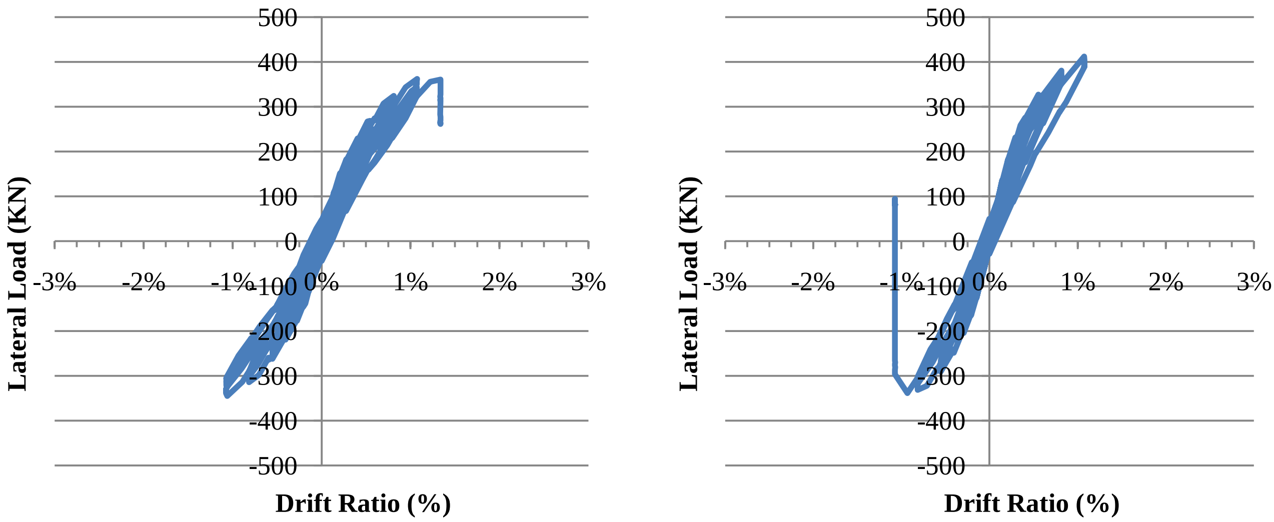

Figure 4. Load-Deflection relationship for Specimens 1 and 2

3.1. Shear Strength

The nominal shear strength of the specimens calculated using several different equations are presented in Table 1. Shear strength provided by the concrete was calculated using expressions for V_c and V_{ci} in the 2008 edition of the ACI 318 Building Code (ACI Committee 318, 2008). The nominal strength was calculated also based on the Modified Compression Field Theory, using the analysis program Response 2000 (Bentz and Collins, 2000). All methods indicated that the specimens were expected to fail due to shear soon after the appearance of flexural shear cracks. The nominal shear force expected to cause yielding of the flexural reinforcement (V_y in Table 1) was calculated based on a moment-curvature analysis. Calculated values of shear strength resulted in ratios of V_n to V_y ranging between 0.56 and 0.86, so the specimens were expected to fail in shear prior to yielding of the flexural reinforcement. Experimental results were consistent with the theoretical values. Measured shear strength was very similar to the values obtained with Eq. 11-4 of the ACI 318 Code.

Table 1. Nominal Strength of Test Specimens

Specimen	*N*	V_{ci}	V_c	V_s	V_n	V_n	V_n	V_y	*Ratio of V_n/V_y*		
		ACI 11-10	ACI 11-4		ACI 11-4	ACI 11-10	MCFT		ACI 11-4	ACI 11-10	MCFT
	KN	KN	KN	KN	KN	KN	KN	KN			
2	1510	154	264	46	311	201	254	360	0.86	0.56	0.71
1	2225	199	305	46	351	245	284	410	0.86	0.60	0.69

Specimens 1 had a maximum shear force of 412 KN in the positive direction of loading (North) and 340 KN in the South direction, while specimen 2 had a maximum shear force of 355 KN in the North direction and 320 in the South (Fig. 3). Measured shear values show that the ratio of nominal shear strength to V_y was close to 1.0.

3.2. Axial Strain

The relationship between drift ratio and axial strain was significantly different for both columns. Both relationships are shown in Fig. 5.

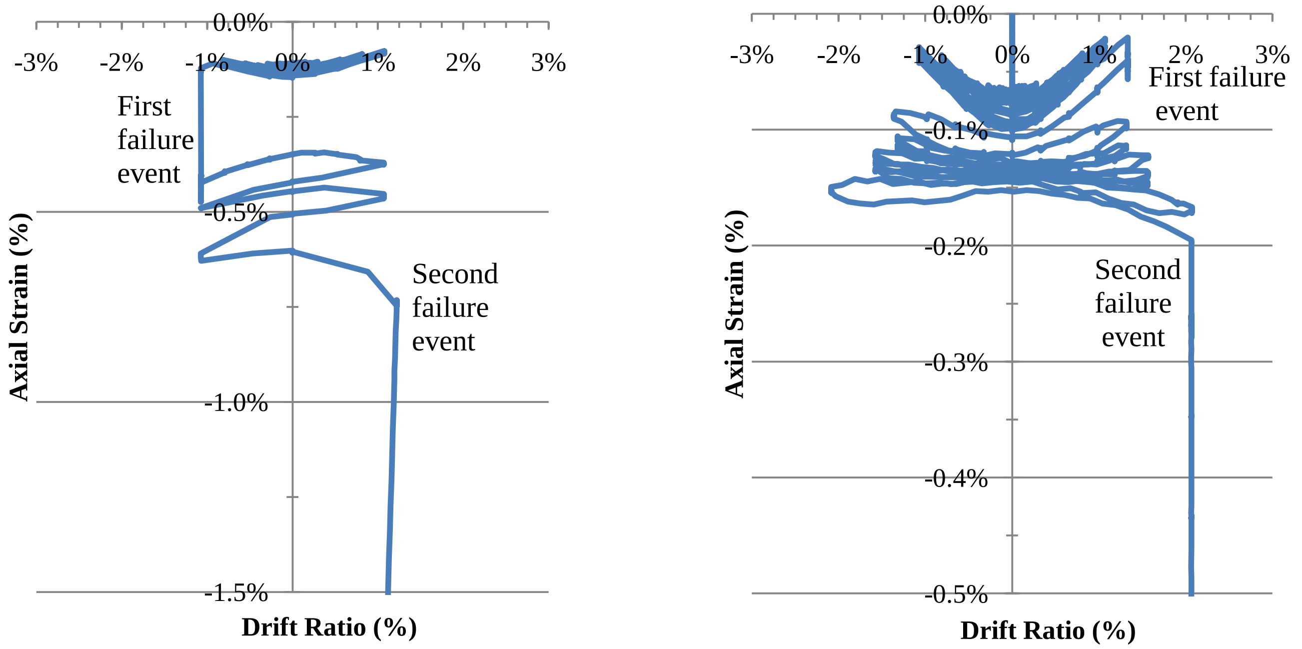

Figure 5. Axial strain vs. drift ratio for specimens 1 and 2.

Figure 5 makes reference to multiple failure events which are tied to events in the loading protocol. As indicated before the control system was set to detect a reduction of 10% or greater on the load carried by the columns. When the trigger limit was exceeded the control system for the vertical actuators shifted from load control to displacement control. This is designated as an axial load failure event. After such an event took place the control system of the vertical actuators was transitioned back to load control, but at the reduced level of axial load at the end of the failure event, and the lateral displacement history resumed. After the second failure event was recorded the columns were loaded monotonically to measure the residual axial capacity.

Figure 5 shows that there was a significant difference between the behavior of the two specimens. Specimen 1, subjected to an axial load of 2225 KN, had a much higher increase in axial strain associated with the first failure event than specimen 2. Furthermore, after the first failure event specimen 1 was able to sustain the reduced level of axial load for a much smaller number of cycles than specimen 2, and the increase in axial strain per cycle was significantly larger than that observed in specimen 2.

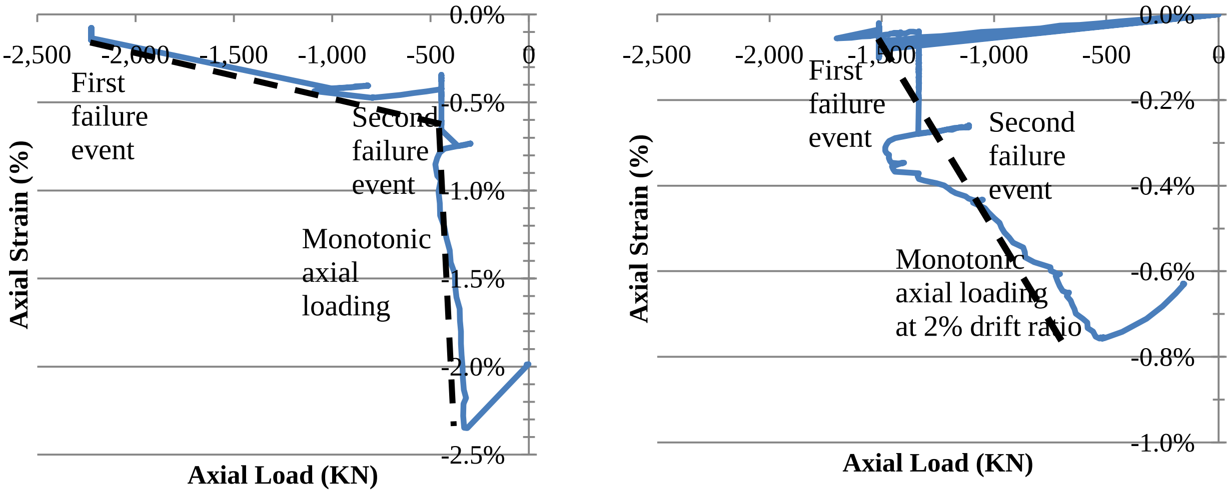

Figure 6. Axial strain vs. axial load for specimens 1 and 2

Figure 6, which shows the relationship between axial strain and axial load for the two specimens, also indicates that there were significant differences in the behavior of the two specimens after the first failure event. The dashed line in both figures represents an approximate failure line for the axial load observed during the tests. In specimen 1 there was a very large reduction in axial load capacity associated with the first failure event. After the first failure event took place in specimen 1, and the control system shifted to displacement control in the vertical actuators, a first attempt was made to increase the axial load in the column. As soon as the axial load reached the failure line, a second failure event occurred. After that, the lateral displacement history was continued at an axial load below the observed failure line. As the column was subjected to deformation cycles in the in the lateral direction, axial strain continued to increase under constant axial load due to further damage to the column. When the axial strain reached the failure line another failure event took place. At this point damage in the column was so severe that the column was loaded monotonically to measure the residual axial capacity.

A similar line is shown in Fig. 6 for specimen 2. A comparison between the two failure lines shows that the slope of the line was significantly higher for specimen 2. Specimen 1 had a very large reduction in axial load capacity associated with the first failure event and maintained a very small residual capacity for subsequent increases in axial strain. In specimen 2 the loss in axial load capacity was much more gradual. After the second failure event the specimen still maintained a significant fraction of its load carrying capacity.

3.3.Lateral Stiffness

One of the goals of the experimental was to improve the ability to simulate the behavior of column elements at drift demands larger than the drift associated with axial failure. The load-deformation response of the two specimens at drift demands beyond axial failure is shown in Fig. 6. The last load cycle prior to axial failure is shown by the dashed lines. The solid lines represent the response of the specimens after axial failure.

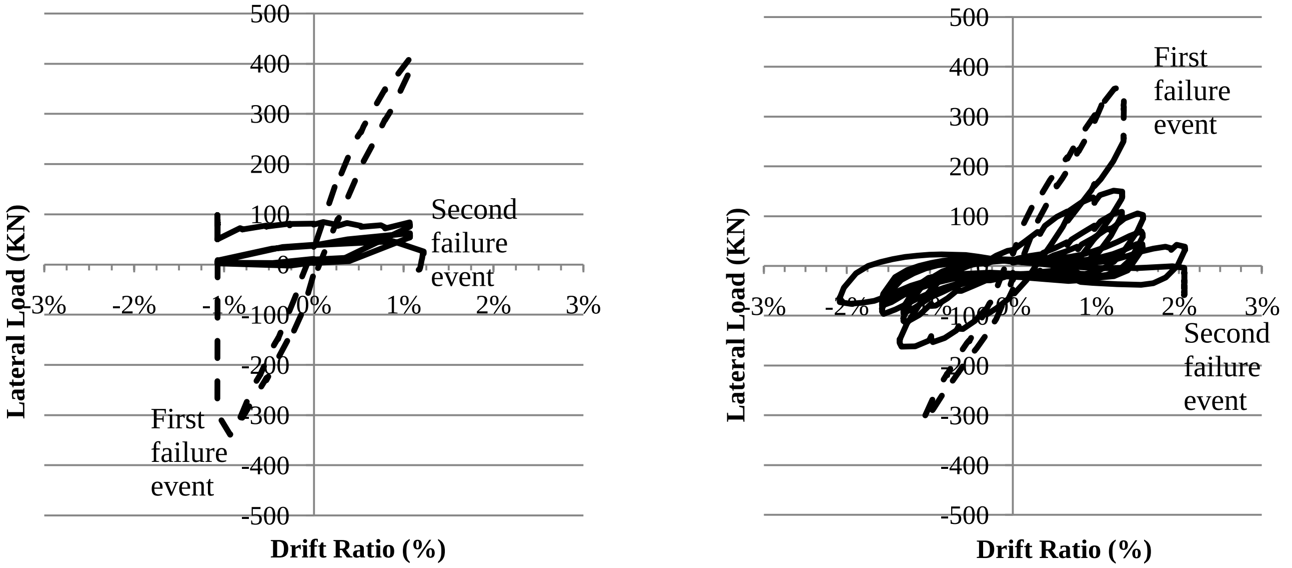

Figure 6. Load-deformation response for specimens 1 and 2 at drift demands beyond axial failure

Figure 6 shows that the behavior of the two specimens was significantly different. Specimen 1 had negligible stiffness after the first failure event, and there was a relatively small increment in lateral drift ratio (to 1.2%) before the column lost its ability to carry the reduced axial load. In the case of specimen 2, the specimen had a very significant reduction in lateral stiffness after the appearance of the shear crack that caused axial failure, but the lateral stiffness was not negligible. Furthermore, there was a very significant increment in the lateral drift ratio before the ability to carry the reduced axial load was lost.

3.4. Behavior at Drift Demands greater than the Drift at Axial Load Failure

The drift ratio measured at each failure event was compared with estimates obtained using the failure model developed by Elwood and Moehle (2005). Results are shown in Fig. 7.

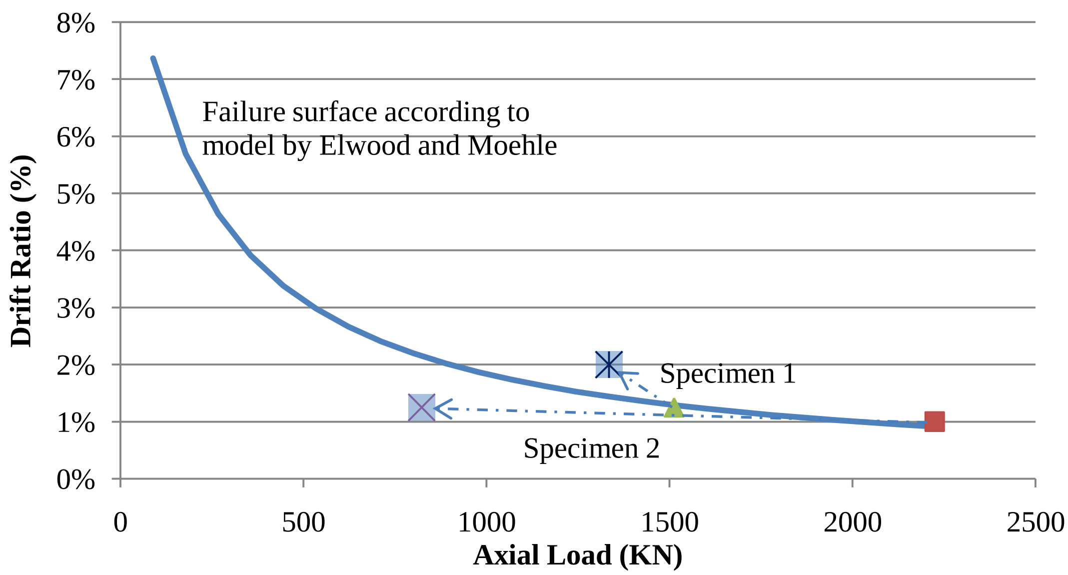

Figure 7. Relationship between drift ratio at axial failure and axial load for multiple failure events.

While the model by Elwood and Moehle (2005) provided a very close match for the first failure event, results were not as good for subsequent failure events. Furthermore, behavior beyond the first failure event was very sensitive to the axial load on the specimen. While the model by Elwood and Moehle overestimated the drift ratio corresponding to the second failure event of specimen 1 (higher axial load), it significantly underestimated the drift ratio corresponding to the second failure event of specimen 2 (lower axial load).

6. SUMMARY AND CONCLUSIONS

The following differences were observed between the two tests. For specimen 1, subjected to a higher axial load of 2225 KN, the axial load stably carried by the column after the first failure event was significantly lower than the load carried by specimen 2. After the first failure event the column was able to carry an axial load of 820 KN, or 37% of the initial axial load. After the first failure event specimen 2, subjected to a lower axial load of 1510 KN, was able to sustain an axial load of 1335 KN, or 88% of the initial axial load.

There was a significant difference in the lateral stiffness of the specimens at drift demands beyond the drift at axial load failure. In specimen 1, which had higher axial load, the lateral stiffness of the column after the first failure event was negligible. This was not the case for specimen 2, in which the lateral stiffness continued to decrease until it became negligible, at which point a second failure event was triggered.

Although the behavior of both specimens may be characterized as significantly brittle, the tests show that the specimen with the lower axial load is more likely to carry a reduced level of axial load after the first failure event. However, this observation is based on pseudo-static tests in which the vertical displacement was controlled to prevent catastrophic collapse of the columns. In real structures the ability of the column to continue to deform with reduced capacity will be dependent on the ability of the floor system to re-distribute some of the axial load to adjacent members, and of the lateral load system to prevent the collapse of the structure when that happens.

7. REFERENCES

ACI Committee 318. (2008). Building Code Requirements for Structural Concrete and Commentary. American Concrete Institute, Farmington Hills, MI. 467 pp.

Bentz, E., and Collins, M. (2000). Response 2000, Reinforced Concrete Sectional Analysis using the Modified Compression Field Theory, University of Toronto, http://www.ecf.utoronto.ca/~bentz/home.shtml

Elwood, K. and Moehle, J., (2005). Axial Capacity Model for Shear-Damaged Columns. *ACI Structural Journal*. 102:4, 578-587.

University of Minnesota, (2008). Multiaxial Subassembly Testing Laboratory. http://nees.umn.edu/index.php

8. ACKNOWLEGMENTS

The authors would like to acknowledge the support provided by the staff from the NEES MAST facility at the University of Minnesota. Our thanks to Carol Shield, Paul Bergson, Angela Kingsley, Jonathan Messier and Drew Daugherty for their contributions to make this a successful testing program. The work of Travis Malone, Emily Reimer and Vinur Kaul was instrumental to the successful fabrication of the specimens. Kurt Henkhaus and Julio Ramirez from Purdue University provided valuable feedback and were actively involved during the planning, instrumentation, and testing of the specimens. Their valuable contributions are gratefully acknowledged. This work was supported primarily by the National Science Foundation under award number # 0618804 through the Pacific Earthquake Engineering Research Center (PEER). Any opinions, findings, and conclusions or recommendations expressed in this material are those of the author(s) and do not necessarily reflect those of the National Science Foundation.